

Seismic performance of a rocking bridge pier substructure with frictional hinge dampers

Chin-Tung Cheng* and Fu-Lin Chen^a

Department of Construction Engineering, National Kaohsiung First University of Science & Technology, No. 1, University Road, Yenchao, Kaohsiung 824, Taiwan

(Received September 18, 2012, Revised August 13, 2013, Accepted September 18, 2013)

Abstract. The rocking pier system (RPS) allows the columns to rock on beam or foundation surfaces during the attacks of a strong earthquake. Literatures have proved that seismic energy dissipated by the RPS through the column impact is limited. To enhance the energy dissipation capacity of a RPS bridge substructure, frictional hinge dampers (FHDs) were installed and evaluated by shaking table tests. The supplemental FHDs consist of two brass plates sandwiched by three steel plates. The strategy of self-centering design is to isolate the seismic energy by RPS at the columns and then dissipate the energy by FHDs at the bridge deck. Component tests of FHD were first conducted to verify the friction coefficient and dynamic characteristic of the FHDs. In total, 32 shaking table tests were conducted to investigate parameters such as wave forms of the earthquake (El Centro 1940 and Kobe 1995) and normal forces applied on the friction dampers. An analytical model was also proposed to compare with the tested damping of the bridge sub-structure with or without FHDs.

Keywords: rocking; self-centering; bridge structure; damping ratio; frictional hinge damper

1. Introduction

Research on the rocking behavior of structures can be dated back to the early work of Housner (1963). Following research by Tso and Wong (1989) pointed out that the response of rigid blocks was largely affected by the size of the blocks. Low frequency vibration, however, was unrelated to the amplitude and coefficient of restitution of materials. Aslam *et al.* (1980) utilized anchored bars to enhance the lateral resistance of rocking structures. Makris and Zhang (2001) investigated the response of anchored rigid blocks under pulse-type motions and found that restrainers were more efficient in preventing overturning if smaller blocks were subjected to low frequency pulses. To assess the seismic response of rocking structures, Priestley *et al.* (1996) developed a practical methodology using standard displacement and acceleration response spectra based on the assumption of representing a rocking block as a single-degree-of-freedom (SDOF) oscillator with constant damping. Their results were then applied in the FEMA 356 document (2000). However, Makris and Konstantinidis (2003) showed that rocking spectra were not identifiable by the

*Corresponding author, Professor, E-mail: ctcheng@nkfust.edu.tw

^a Graduate Student

response spectra of a SDOF oscillator and recommended a damping ratio for rocking structures.

Mander and Cheng (1997) theoretically evaluated the radiation damping of the rocking bridge pier due to the energy loss during column impact on beam surfaces. This damping behavior can also be found in the context of wave propagation through the soil under the structural foundation. Cheng (2007) studied the impact behavior of free or anchored columns through quick release tests. It was found that damping prediction for rocking columns with slenderness (height vs. width) 4 or 6 agreed well with the test results. Cheng (2008) also investigated the seismic performance of an RPS bridge sub-structure through shaking table tests. Test results showed that the rocking structure only dissipated limited energy.

Tests proved that RPS behaved linear elastically without residual displacement, which is also referred to as self-centering structures. Recently, self-centering relative research was extensively proposed in the area of bridges (Lee and Billington 2011, Guo *et al.* 2012, Kim *et al.* 2010), bracing systems (Zhu and Zhang 2008, Christopoulos *et al.* 2008) and shear walls (Clayton *et al.* 2011) etc. In these literatures, energy dissipation devices were introduced to minimize seismic response of the self-centering structures. Similarly, in this research, frictional hinge dampers (FHDs) are added to enhance the seismic performance of the self-centering bridge structure. The friction-viscoelastic damping system had been proposed by Nielson *et al.* (2004) for the energy dissipation of the isolated structure. Morgan *et al.* (2004) utilized friction damper in the beam column joint of precast structures. These dampers consisted of brass plate sandwiched by steel plates, and they were connected by the steel rods and prestressed to apply normal force. The dampers dissipate energy in a passive way whenever an earthquake initiates any inter-storey drift in the structures.

2. Thoretical models

Based on the research of Mander and Cheng (1997) and Cheng (2007, 2008), the radiation damping of a self-centering designed bridge may be derived as follows. As shown in Fig. 1, the cap beam and columns in a self-centering designed bridge may be precast and constructed separately, then connected together by unbonded post-tensioned tendons inside the columns. The slack or post-tensioned tendons provide stability, ductility and a restoring force for the bridge. Due to the use of special detailing in the beam-column interfaces, the structures may behave in a bilinear elastic manner without inducing any damage. If tendons are snugly tightened, the tensile force in the tendons, f_s , may be calculated as

$$F_s = A_s f_s = K_s \theta \leq A_s f_y \quad (1)$$

in which $K_s = E_s A_s \left(\frac{b}{L_T}\right)$ is rotational stiffness of columns provided by tendons, E_s elastic modulus of tendons, A_s the area of tendons, f_s tensile stress of tendons, f_y yielding strength of tendons, L_T the anchorage length of tendons, θ the rotation of columns, and b is the width of the columns. Before rocking, the stiffness of columns under seismic loads is

$$K_c = n_c \frac{12EI_{eff}}{H_c^3} \quad (2)$$

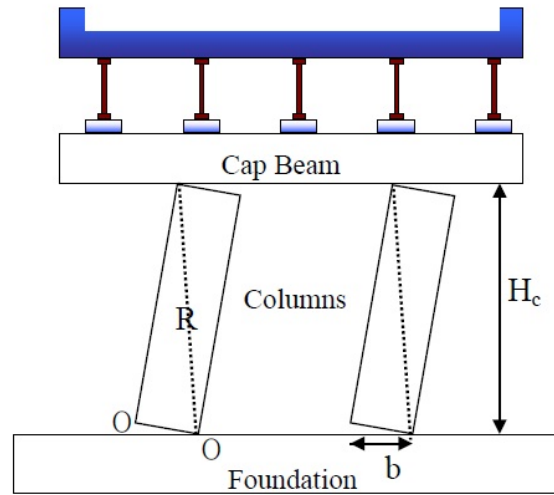


Fig. 1 Rocking behavior of a self-centering designed bridge

where n_c is the number of columns in the bridge substructure, H_c the height of columns, E elastic modulus of the column material, I_{eff} effective moment of inertia, which is $0.5 I_g$ for reinforced concrete columns and $0.7 I_g$ for prestress and precast columns, and I_g the moment of inertia for a gross section of columns. The base shear coefficient before column rocking can be expressed as

$$C_c = \frac{F}{W} = \frac{K_c \Delta}{W} \tag{3}$$

where F is the lateral force at the top of columns, W the total weight of the bridge superstructure, and Δ the lateral displacement at the top of columns. The base shear coefficient after column rocking can be expressed as

$$C_c = \frac{F}{W} = \frac{b - \Delta}{H_c} + n_c \frac{K_s}{W} \frac{b}{H_c} \frac{\Delta}{H_c} \leq \frac{b - \Delta}{H_c} + n_c \frac{A_s f_y b}{WH_c} \tag{4}$$

If the rotational stiffness of columns with respect to the base is defined as

$$r_s = \frac{n_c E_s A_s}{W} = \frac{n_c K_s L_T}{W(b)} \tag{5}$$

and letting $\theta = \frac{\Delta}{H_c}$, then Eq. (4) can be rewritten as

$$C_c = \frac{b}{H_c} \left[1 - \left(\frac{H_c}{b} - r_s \frac{b}{L_T} \right) \theta \right] \leq \frac{b}{H_c} \left[1 - r_s \varepsilon_y - \frac{H_c \theta}{b} \right] \quad (6)$$

The seismic energy is dissipated through each impact of column rocking. If the impact is assumed to be inelastic without bounce, the reduction factor of kinetic energy is found by equating the moment of momentum prior to and after the impact. Before the impact, the bridge deck and cap beam move in a rigid body motion with a translation velocity, which has a downward component. As shown in Fig. 1, the moment of momentum with respect to rocking toe O can be calculated as

$$I_{bf} = I_{bdg} \left[1 - \frac{n_c m_c b^2 / 2 + m_d b^2}{I_{bdg}} \right] \dot{\theta}_{bf} \quad (7)$$

where $I_{bdg} = I_c + I_d$, I_c and I_d are the moment of inertia for the columns and deck with respect to rocking toe O, respectively. After the impact, the bridge deck and cap beam also travel in rigid body motion with a translation velocity, including an upward component. The moment of momentum with respect to rocking toe O' can be calculated as

$$I_{af} = I_{bdg} \dot{\theta}_{af} \quad (8)$$

By equating the moment of momentum prior to the impact in Eq. (7) and after the impact in Eq. (8), the kinetic energy reduction factor can be defined as

$$r = \frac{\frac{1}{2} I_{bdg} \dot{\theta}_{af}^2}{\frac{1}{2} I_{bdg} \dot{\theta}_{bf}^2} = \left(\frac{\dot{\theta}_{af}}{\dot{\theta}_{bf}} \right)^2 = \left[1 - \frac{n_c m_c b^2 / 2 + m_d b^2}{I_{bdg}} \right]^2 \quad (9)$$

The radiation damping can be evaluated from the energy dissipated in each impact on half-cycle as

$$\xi_{eq} = \frac{\delta E}{\pi F \Delta} = \frac{E_P (1 - r)}{\pi F \Delta} \quad (10)$$

where δE is the energy loss due to impact and E_P potential energy, which is restored in the increase of the elevation in the centroid and the strain energy in tendons, can be expressed as

$$E_p = Wb\theta \left[1 + r_s \left(\frac{b\theta}{2L_T} \right) \right] \quad (11)$$

Substituting Eqs. (6) and (11) into (10), the radiation damping may be expressed as

$$\xi_{eq} = \frac{(1-r)}{\pi} \frac{[1 + r_s (\frac{b\theta}{2L_T})]}{[1 - (\frac{H_c}{b} - r_s \frac{b}{L_T})\theta]} \quad (12)$$

If the structure installed with the FHDs as shown in Fig. 2, the equivalent damping ratio of the

rocking structure can be expressed as

$$\xi_{eq} = \frac{\delta E}{\pi F \Delta} \tag{13}$$

where F and Δ are lateral force and displacement at the deck, respectively, δE = energy dissipated by the FHDs in a half cycle which can be expressed as

$$\delta E_p = 2M\theta \tag{14}$$

in which M is moment of FHDs with respect to the center of the mass at the deck, and θ rotation angle of FHDs in quarter cycle. Assuming the normal force is uniformly distributed over the area of a brass plate, the moment resistance of the FHDs with respect to the deck can be calculated as

$$M = n \int_0^r \mu \frac{N}{\pi r^2} dA \cdot \rho = n \mu \frac{N}{\pi r^2} \int_0^r 2\pi \rho d\rho \cdot \rho = \frac{2}{3} \mu N n r \tag{15}$$

Where μ is friction coefficient between the brass and steel plates, N normal force applied to the FHDs, n numbers of surface providing the friction force, and r is outside diameter of circular brass plates.

For the structure tested in this research, the effective damping is made up of equivalent damping plus inherent viscous damping, ξ_{in} which exists in any structures vibrating in the elastic range. The inherent viscous damping may range from 2% to 5%, but was set to be 3% for a simple structure without any cracks observed in the test. The equivalent damping comes from friction damping or radiation damping for structures with or without the damper, respectively. Therefore, the effective damping for the bridge structure is expressed as

$$\xi_{eff} = \xi_{in} + \xi_{eq} \tag{16}$$

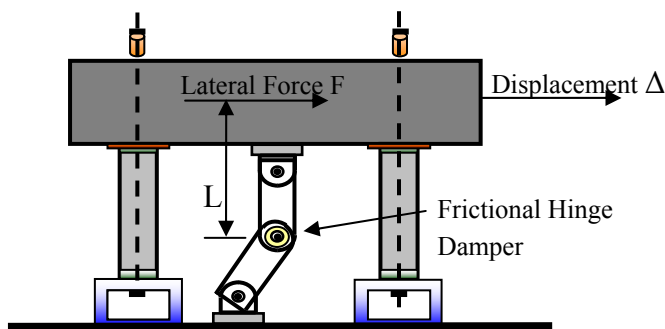


Fig. 2 Lateral resistance of a self-centering designed bridge

3. Experimental programs

The test program was preceded by measuring the friction coefficient between brass and steel plates, followed by the component test of FHDs and finally performed shaking table tests of the bridge structure installed with or without FHDs. The friction coefficient between the steel and brass plates was measured to be 0.19 by the static test of a material test machine. Fig. 3 shows the test setup and partial results of the component test of FHDs. The supplemental FHD consists of two 150 mm circular brass plates sandwiched by three rectangular steel plates all connected by a 22 mm diameter high strength bolts as shown in Fig. 3(a). Between the nut and steel plates, a load cell was installed to measure the normal force applied on the FHDs. The size of central steel plate is 1150*200*19 mm and the size of the other two rectangular steel plates is 600*200*19 mm. As shown in Fig 3(a), a 100 kN actuator applies the lateral force to the FHD in a way of displacement control to investigate its dynamic performance in terms of the loading displacement, normal force on the FHD, loading frequency and cycles. Test results show that energy dissipation of the FHD increases with the increase of the displacement and normal force applied on the FHD, however, decreases with the increase of the loading frequency as shown in Fig. 3(b).

Then two sets of the FHD were installed in parallel between the bridge deck and shaking table as shown in Fig. 2. The concrete block 3000x1000x450 mm in size weighed 2920 kg, representing the cap beam and bridge deck as shown in Fig. 4. The columns 300x300x1200 mm in size were longitudinally reinforced with eight D16 (Grade 60, $f_y = 414\text{MPa}$) deformed rebars and transversely with D13 Grade 60 rebar spaced 200 mm. To protect the column concrete from crushing during rocking, longitudinal rebars were all fillet-welded to a 2.2 cm thick steel plate at both column ends. To form the steel on a steel rocking interface, a 450x450x22 mm steel plate, seating on the top of the columns, was attached to the bottom surface of the concrete block by four 25 mm bolts. Each column was installed on the 50 mm thick tube wall of a 530x400x200 mm rectangular steel tube. This steel base not only provides the space for the anchorage of unbonded high strength steel bar passing through the columns but also transfers the column shear to the shaking table through four 40 mm bolts. A D22 high strength ($f_y = 1100\text{MPa}$) threaded bar in each column snugly connects the concrete deck, precast columns and steel bases together. Since the anchorage length of unbonded high-strength threaded bar in the model bridge seems too short to let the columns rock, the application of disc springs on the anchorage zone of the high strength bars at the deck provides appropriate angular stiffness similar to the full-sized bridge as well as extra deformation capacity for the bridge model under the excitation of strong ground shaking. A disc spring with outside diameter 125 mm, inside diameter 61 mm and 5 mm thick may have compressive stiffness of 11333 kN/m and allowable compressive displacement of 4 mm. Two Maxwell series composition of eight springs in one D22 steel bar per column results in total stiffness of 5566 kN/m and an allowable compressive displacement of 32 mm. Based on this spring stiffness, the rotational stiffness of columns with respect to the base shear, r_s , calculated by Eq. (5) is 330, which is similar to the full-sized bridge and significantly reduced from 4430 for columns anchored by a single D22 high strength threaded bar without disc springs. To prohibit the column slips, the baffle board was installed at the column ends. It is noted that there is 2 mm gap between the baffle board and columns that allows columns to rock. The concrete strength at test days for columns and block was measured to be 29.6 MPa and 24.1 MPa, respectively.

Before tests, two accelerometers were installed on the shaking table and concrete deck as shown in Fig. 5. In addition, four temposonic linear transducers measured the deck displacement

and column rotations. Load cells at the two FHDs monitored the variation of normal force during the column rocking. In total, 32 shaking table tests were conducted. Table 1 summarizes the structural response of the tests. The first character “N, A, B and C” in the test identification represents the normal force applied on the FHDs such as 0, 900kg, 1400 kg and 1800 kg. The second character “E and K” means wave form of excitations such as El Centro in 1940 and Kobe in 1995. The last group of three numbers indicates the levels of ground shaking in gal (1g=1000 gal). Fig. 6 illustrates structural response of a typical shaking table test including table acceleration, displacement and acceleration at the deck, and effective damping evaluated by a modified elastic response spectra.

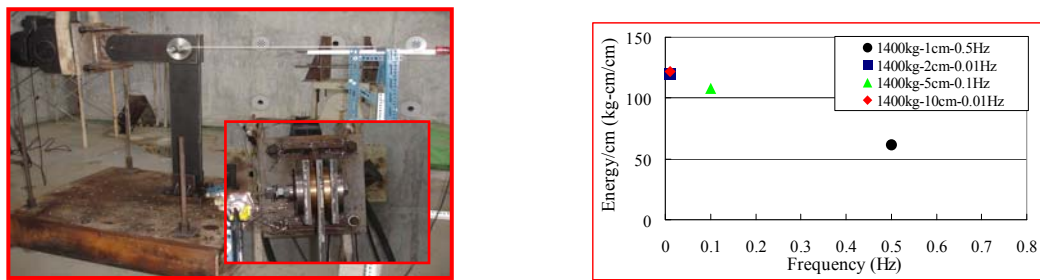


Fig. 3 Component tests of FHD

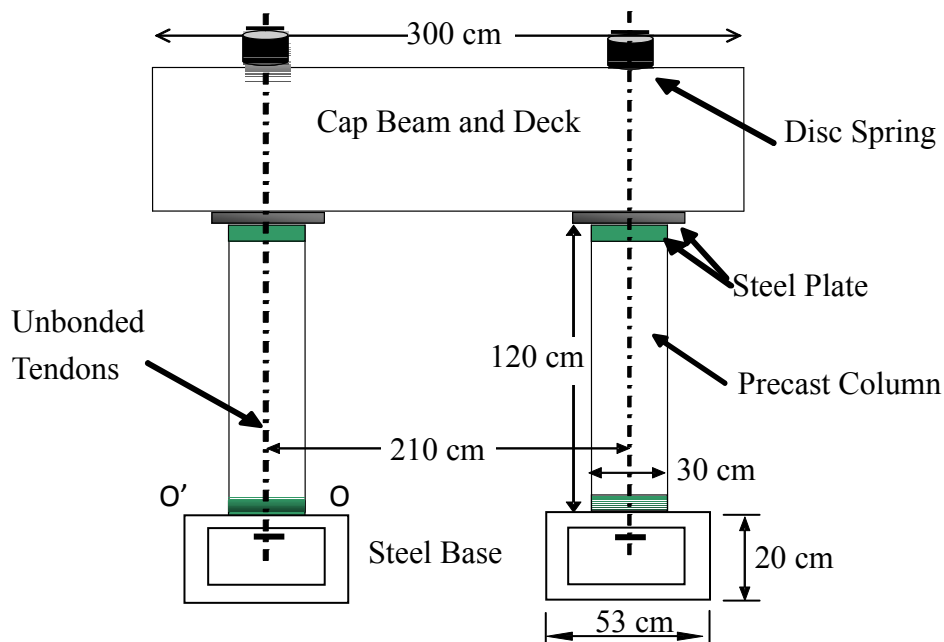


Fig. 4 Details of a self-centering designed bridge model

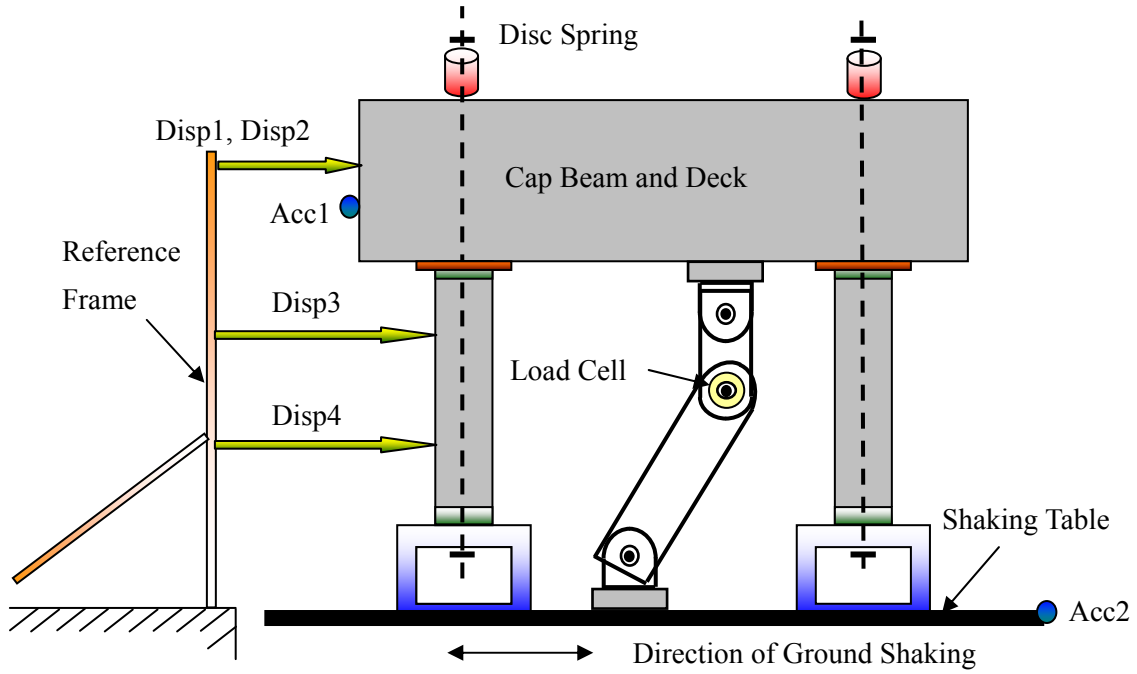


Fig. 5 Test setup and measurements of the bridge model

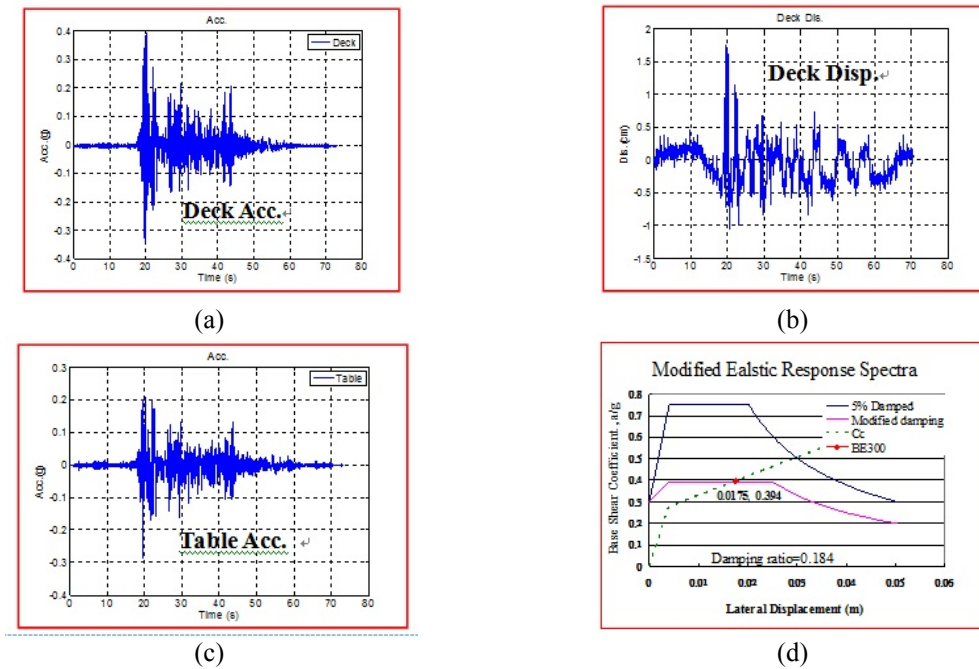


Fig. 6 Structural response of a typical test BE300

Table 1 Summary of structural response of the tests

Test	Table-acc (gal)	Deck-acc (gal)	Deck-disp (cm)	Rotation (rad)	Tested Damping	Analytical Damping
AE100	106	126	0.467	0.006	0.198	0.065
AE200	232	230	1.162	0.007	0.236	0.054
AE300	283	443	1.686	0.012	0.146	0.049
AE400	352	577	1.938	0.013	0.152	0.048
BE100	105	153	0.603	0.007	0.134	0.079
BE200	212	266	2.686	0.007	0.082	0.052
BE300	286	394	1.751	0.009	0.184	0.059
BE400	349	477	2.741	0.012	0.220	0.052
CE100	100	139	1.091	0.005	0.106	0.079
CE200	211	251	1.188	0.006	0.200	0.077
CE300	274	382	1.740	0.010	0.194	0.068
CE400	319	485	2.392	0.013	0.210	0.061
AK100	103	108	0.568	0.006	0.270	0.062
AK200	195	236	0.751	0.007	0.226	0.059
AK300	326	564	1.583	0.010	0.089	0.050
AK400	512	1050	3.276	0.024	0.046	0.042
BK100	103	109	1.925	0.008	0.264	0.058
BK200	211	219	1.577	0.008	0.260	0.061
BK300	284	575	1.871	0.013	0.086	0.058
BK400	432	877	3.057	0.017	0.065	0.050
CK100	101	100	0.603	0.005	0.320	0.094
CK200	194	194	0.811	0.005	0.330	0.087
CK300	306	546	1.566	0.013	0.094	0.070
CK400	430	848	2.643	0.023	0.070	0.059
NE100	98	214	1.321	0.005	0.038	0.057
NE200	193	369	1.337	0.006	0.092	0.053
NE300	281	478	1.007	0.007	0.122	0.052
NE400	351	571	1.587	0.011	0.154	0.050
NK100	125	275	1.366	0.009	0.024	0.057
NK200	273	639	2.770	0.016	0.018	0.053
NK300	355	946	2.958	0.020	0.032	0.052
NK400	487	1219	3.917	0.030	0.034	0.050

Note: N: without FHD, A: FHD with 900 kg normal force, B: FHD with 1400 kg normal force, C: FHD with 1800 kg normal force, E: El Centro Earthquake, K: Kobe Earthquake, number 400: intensity level of ground shaking in 400 gal

Visual observation of all tests revealed that the beam–column interface remained in contact until excitations exceeded 200 gal. When the columns started to rock, the deck moved in rigid body motion and the bridge returned to its original position after the excitations without damage or any sign of residual deformations. As shown in Table 1, the bridge with or without FHDs rocked up to 2.3% and 3.0% drift under the excitation of 400 gal ground shaking, respectively. In order to understand the dynamic characteristic of bridges, a Fast Fourier Transform (FFT) was applied to the deck acceleration of the bridge for some typical tests as shown in Figs. 7 and 8. It is seen that the bridge vibrated in a fundamental frequency in response to the broader spectrum of the shaking table in all tests. The fundamental frequency for the bridge without FHDs slightly decreases with the increase of increasing intensity of ground shaking, however, it remained the same for the bridge applied with FHDs as shown in Fig. 8. It is evident that adding stiffness by FHDs let the bridge vibrate in a particular fundamental frequency, regardless of the increase in ground shaking.

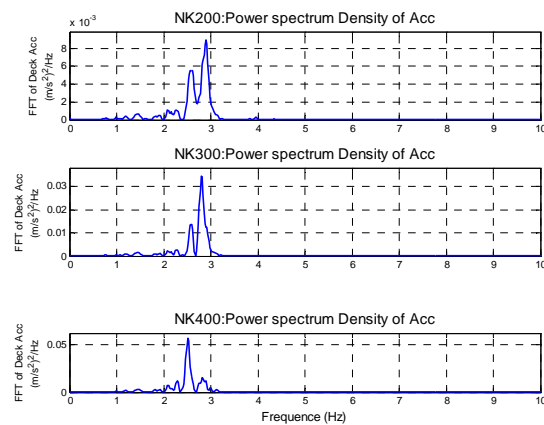


Fig. 7 Frequency spectrum of a bridge response without FHD under ground excitation of increasing intensity

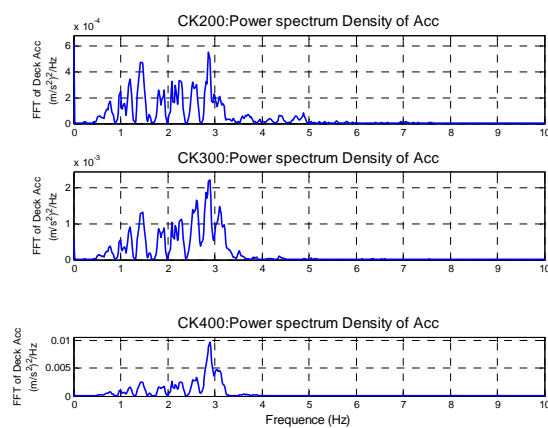


Fig. 8 Frequency spectrum of a bridge response with FHD under ground excitation of increasing intensity

4. Damping evaluations

Self-centering structures without FHDs dissipate energy through the column impact, however, self-centering structures with FHDs dissipate the energy through the friction. It is evident that the radiation damping of rocking structures cannot be evaluated from hysteretic loops, unlike the conventional structures that dissipate energy through plastic deformations. To experimentally estimate the damping due to the column impact, a procedure proposed by the ATC (1995) is illustrated in Fig. 6(d), where a 5% damped response spectra can be reduced by a higher damping. Therefore, the reduction factor of the base shear coefficient for the short period can be expressed in terms of a higher damping ratio as

$$B_s = \left(\frac{\xi}{0.05} \right)^{0.5} \tag{17}$$

and similarly for the long period

$$B_l = \left(\frac{\xi}{0.05} \right)^{0.3} \tag{18}$$

Therefore, the base shear for the short period due to higher damping is modified as

$$C_d = 2.5 \frac{A}{B_s} \tag{19}$$

and similarly for the long period

$$C_d = \frac{SA}{TB_l} \tag{20}$$

As shown in Fig. 6(d), the point of measured peak acceleration versus relative displacement at the concrete deck was first illustrated along with 5% damped response spectra. To match the response spectra to the test result, a higher damping of 18.4% was used to modify it based on Eqs. (17) or (18), as appropriate. From the figure, it can be seen that the test result is also not far from the performance point where the pushover capacity of the bridge (dotted line) and modified base shear demand curve intersect. Following this procedure, tested damping ratios for bridges are summarized in Table 1. It can be seen that experimental damping ratios for the bridge applied with and without FHDs range from 4.6% to 27% and 3.4% to 15.4%, respectively. Fig. 9 illustrates the structural response of the bridge installed with or without the FHDs. In Figs. 9(b) and 9(e), a thick straight line (2.5A) was plotted to represent maximum amplification of the ground acceleration at the bridge deck. Compared with the performance of the bridge installed with or without FHDs, it is found that FHDs effectively reduce the displacement and acceleration at the deck, while increasing the damping ratios of the structure. The larger the normal force applied on FHDs, the more significant the effect of the FHDs is. As shown in Table 1, the tested damping ratios for the structure without FHDs average to be 0.06, while it increased to 0.19 for the tests applied with 1800 kgf normal force on FHDs. This fact manifests that FHDs can enhance the seismic performance of self-centering designed bridge structure. It is also noted that the bridge applied with FHDs and excited by the ground shaking less than 200 gal intensity was hard to rock and vibrated in a very high frequency within the ascending branch of the response spectra as shown in

Fig. 6(d), leading to an unreasonably high damping estimated by the response spectra.

Fig. 9(c) shows the comparison of analytical and tested damping ratios for the bridge applied without the FHDs, while it is illustrated in Fig. 10 for the bridge with FHDs. Where analytical damping ratios were calculated by adding a 3% inherent viscous damping to the equivalent damping based on Eq. (16). Without FHDs, the bridge dissipates energy through column impact at the deck or foundation surfaces. As shown in Fig. 9(a) to 9(c), it is found that the structure excited by the Kobe earthquake (near fault) seems to have larger displacement and acceleration at the deck than those excited by El Centro earthquake (free field). And the proposed theory slightly overestimates the damping ratios for the structure excited by the Kobe earthquake, while significantly underestimates the tested damping for the structure excited by the El Centro earthquake with the damping increasing with the increase of the intensity level of ground shaking, as shown in Fig. 9(c).

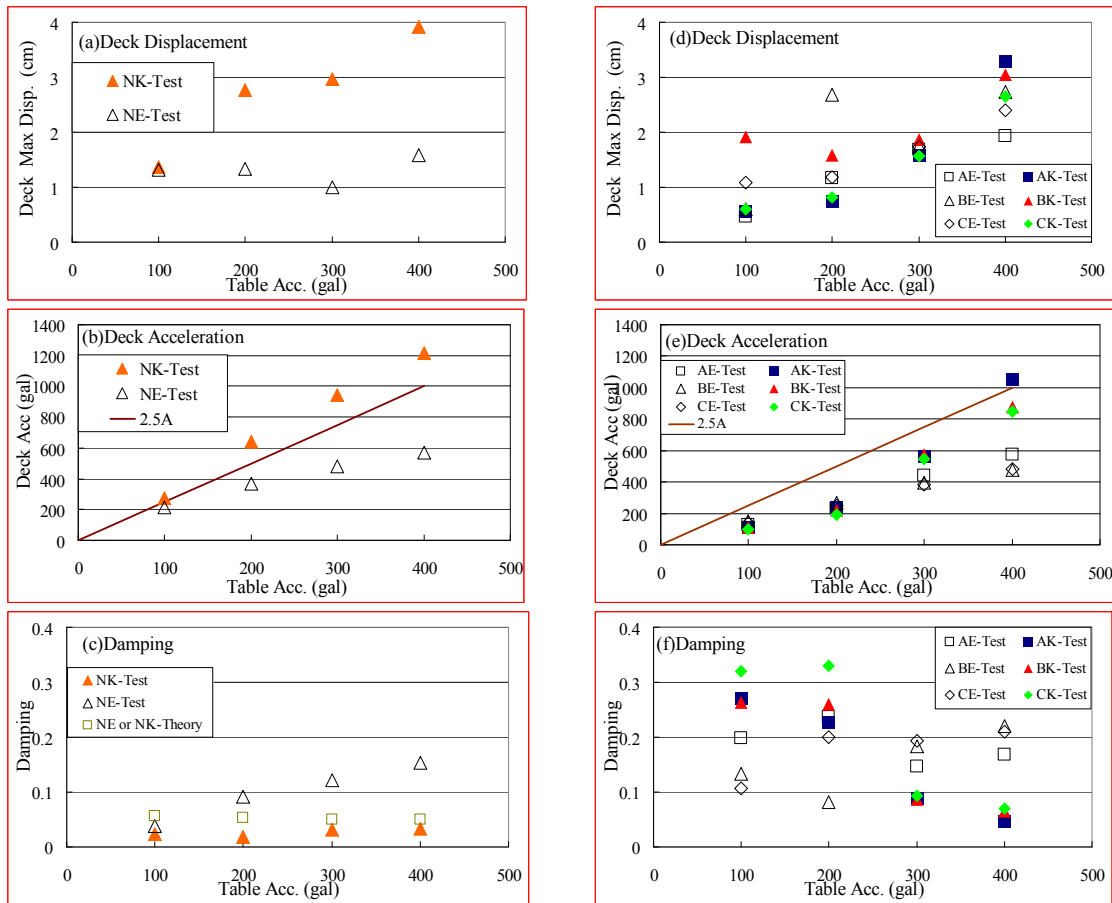


Fig. 9 Structural response of the bridge installed with or without FHD

With FHDs, the bridge relies on energy dissipation by the friction of FHDs to enhance its seismic performance. As shown in Fig. 9, it is found that the FHDs effectively reduce displacement and acceleration at the deck but increase the damping. It is noted that the tested damping decreased with the increase of deck displacement and acceleration for the bridge excited by the Kobe earthquake. This fact is found similar to the study of Cheng (2008), where bridges excited by the Kobe Earthquake pulse-type motion with increasing ground acceleration level had larger deck displacement to reduce the disadvantageous effects such as column slips (2 mm gap), leading to a decrease of the damping ratio when compared with those excited by the El Centro Earthquake. To compare the analytical results as shown in Fig. 10, most tested damping ratios were underestimated by the proposed analytical model, except for the bridge excited by Kobe-earthquake with intensity level of ground shaking larger than 300 gal. Therefore, when the bridge vibrated in a significant rocking motion, its tested damping agrees well with predicted model.

Fig. 11 illustrates the hysteretic relations of displacement versus inertia force of the deck of the bridge for a typical test. As seen in this figure, little energy is dissipated in the elastic hysteretic loops. Based on the area in the hysteretic loops, damping ratio can be evaluated using Eq. (13).

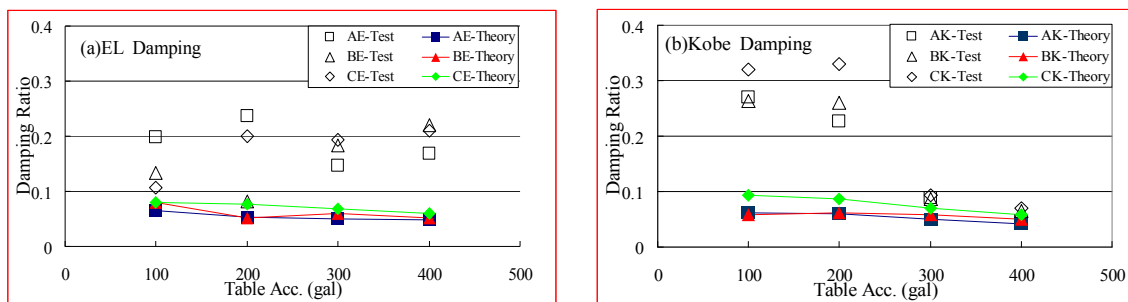


Fig. 10 Analytical and experimental damping ratios for bridges with FHD

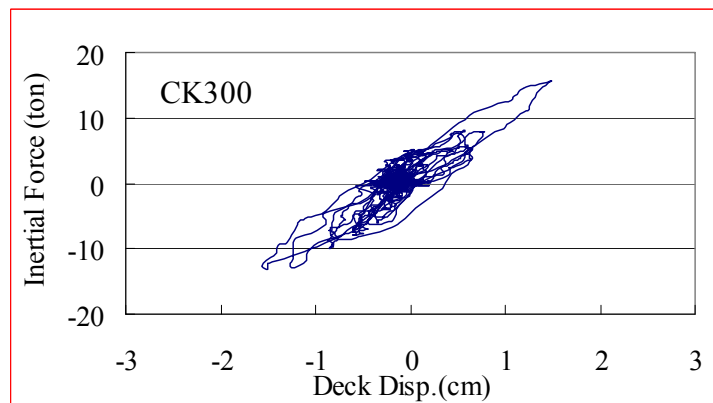


Fig. 11 Hysteretic response of a typical test CK300

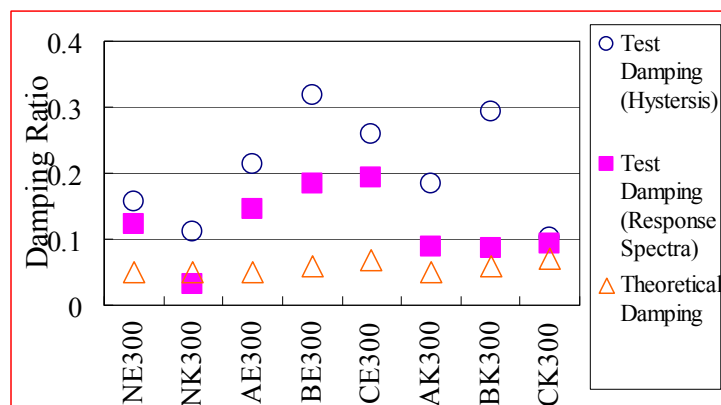


Fig. 12 Experimental damping ratios by hysteresis and response spectra

Fig. 12 shows the comparison of damping ratio evaluated from hysteresis, elastic response spectra and the analytical model. It can be seen that all damping ratios from hysteresis are larger than those obtained from elastic response spectra and the analytical model. All data manifest that the proposed model is conservative in the evaluation of damping ratio for self-centering designed bridges.

5. Conclusions

Frictional hinge dampers were applied to enhance the seismic performance of a self-centering designed bridge sub-structure that can eliminate residual deformations after earthquakes. Based on the FFT analyses, the self-centering structure without FHDs vibrated in a fundamental frequency slightly decreased with increasing intensity of ground shaking, however, vibrated in a particular fundamental frequency with the addition of FHDs. The tested damping was determined from a modified response spectra. The analytical damping of the bridge model was evaluated from the superposition of a 3% inherent damping and the equivalent damping of the bridge system due to the column impact or friction, respectively. Test results show that FHDs effectively reduce the displacement and acceleration at the deck, while increasing the damping ratios of the structure. The bridge applied with or without FHDs rocked up to 2.3% and 3.0% column rotation under the excitation of 400 gal ground shaking, respectively. The tested effective damping ratios for the structure without FHDs average to be 0.06, while it increased to 0.19 for the tests applied with 1800 kg normal force on FHDs. All data manifest that the proposed model is conservative in the evaluation of damping ratio for self-centering designed bridges with FHDs. However, when the self-centering bridge vibrated in significant rocking motion, its tested damping agrees well with predicted model.

Acknowledgements

Financial supports from the National Center for the Research on Earthquake Engineering (NCREE) and National Science Council in Taiwan, with the grant NSC95-2625-M-327-003 are highly appreciated. The authors would like to thank Mr. Shih-Way Yeh for his assistance with the experiment.

References

- Applied Technology Council. (1995), *Guidelines and commentary for the seismic rehabilitation of buildings*, Project ATC-33, Redwood City, California.
- Aslam, M., Godden, W.G. and Scalise, D.T. (1980), "Earthquake rocking response of rigid blocks", *J. Struct. Eng. - ASCE*, **106**(2), 377-392.
- Cheng, C.T. (2007), "Energy dissipation in rocking bridge piers under free vibration tests", *Earthq. Eng. Struct. D.*, **36**, 503-518. (DOI: 10.1002/eqe. 640).
- Cheng, C.T. (2008), "Shaking table tests of self-centering designed bridge sub-structures", *Eng. Struct.*, **30**(12), 3426-3433.
- Christopoulos, C, Tremblay, R. Erochko, J. and Choi, H. (2008), "Response of 2-d and 3-d buildings incorporating buckling-restrained and self-centering bracing systems", *Proceedings of the Annual conference-Canada Society for Civil Engineering*.
- Clayton, P.M., Dowden, D.M., Purba, R. Berman, J.W., Lowers, L.N. and Bruneau, M. (2011), "Seismic design and analysis of self-centering steel plate shear walls", *Proceedings of the Structures Congress 2011- structures congress*.
- FEMA 356. (2000), *Pre-standard and commentary for the seismic rehabilitation of buildings*, Prepared by the American Society of Civil Engineering for the Federal Emergency Management Agency. FEMA, Washington, DC.
- Guo, J., Xin, K., Wu, W. and He, M. (2012), "A simplified model and experimental response of self-centering bridge piers with ductile connections", *Adv. Mater. Res.*, **446-449**, 1036-1041.
- Housner, G.W. (1963), "The behavior of inverted pendulum structures during earthquakes", *B. Seismol. Soc. Am.*, **53**(2), 403-417.
- Kim, T.H., Lee, H.M., Kim, Y.J. and Shin, H.M. (2010), "Performance assessment of precast concrete segmental bridge columns with a shear resistant connecting structure", *Eng. Struct.*, **32**(5), 1292-1303.
- Lee, W.K. and Billington, S.L. (2011), "Performance based earthquake engineering assessment of a self-centering post-tensioned concrete bridge system", *Earthq. Eng. Struct. D.*, **40**(8), 887-902.
- Makris, N. and Zhang, J. (2001), "Rocking response of anchored blocks under pulse-type motions", *J. Eng. Mech. - ASCE*, **127**(5), 484-493.
- Makris, N and Konstantinidis, D. (2003), "The rocking spectrum and the limitations of practical design methodologies", *Earthq. Eng. Struct. D.*, **32**, 265-289.
- Mander, J.B. and Cheng, C.T. (1997), *Seismic resistance of bridge piers based on damage avoidance design*, Technical Report NCEER 97-0014; Buffalo, NY.
- Morgen, B.G. and Kurama, Y.C. (2004), "A friction damper for post-tensioned precast concrete beam-to-column joints", *Proceedings of the 13th World Conference on Earthquake Engineering*, Vancouver, B.C., Canada, August 1-6, 2004.
- Nielsen, L.O., Mualla, I.H. and Iwai, Y. (2004), "Seismic isolation with a new friction-viscoelastic damping system", *Proceedings of the 13th World Conference on Earthquake Engineering*, Vancouver, B.C., Canada, August 1-6, 2004.
- Priestley, M.J.N., Seible, F. and Calvi, G.M. (1996), *Seismic design and retrofit of bridges*, John Wiley and Sons, Inc., New York.

- Tso, W.K. and Wong, C.M. (1989), "Steady state rocking response of rigid blocks part 1: Analysis", *Earthq. Eng. Struct. D.*, **18**, 89-106.
- Zhu, S. and Zhang, Y. (2008), "Seismic analysis of concentrically braced frames systems with self-centering friction damping braces", *J. Struct. Eng. - ASCE*, **134**(1), 121-131.

CC